Seventh Canadian Masonry Symposium
McMaster University
Hamilton, Ontario
June 4-7, 1995

CREEP EFFECTS ON UNREINFORCED SLENDER CONCRETE BLOCK WALLS

Ayman A. Maksoud[1] and Robert G. Drysdale[2]

ABSTRACT

The capacities of slender concrete block walls under sustained eccentric axial loads were investigated using the finite element method.The finite element model accounts for the inelastic material responses, P-δ effects, and time-dependent (creep) strains. Creep functions developed from test data for normal weight masonry prisms were used in the numerical model. Loading and geometric parameters are included in the study. Sustained loads in the range of service loads were kept constant for a period of 25 year after which a short term loading was applied to the walls to investigate the residual wall capacities. Considerable reductions in the short term capacities was found as a result of the long duration of the load.

INTRODUCTION

Back ground

Creep and other time dependent strains in the constituent materials of a symmetric concentrically loaded unreinforced masonry wall do not change the capacity. This is because, they cause only additional shortening of the wall without producing additional internal stresses or stress redistributions. For reinforced masonry sections under concentric axial loads, stress redistributions take place between the masonry material and the reinforcement, usually resulting in higher capacities (Ben-Omran et al., 1989). Sections subjected to initial out-of-plane bending resulting from eccentric axial load have nonuniform stress distributions across the wall leading to corresponding variations in creep strains and increased curvature. The added creep curvature results in additional wall deflection. For stocky members, creep deflections are generally insignificant but, for slender members, the additional P-δ effect due

1 Assistant professor, Civil Engineering, Ain-Shams University, Cairo Eqypt

2 Professor, Civil Engineering, McMaster University, Hamilton, Ontario, L8S 4L7

to creep deflection may produce significant additional internal stresses due to the increased moment. Therefore, the creep effect cannot be neglected in determining the capacities of slender walls.

Shrinkage and thermal movements are other potential sources of wall deflections. However, to the extent that these deformations are uniform across the wall section, which is the case for shrinkage and constant surrounding temperature for unreinforced masonry walls, no additional lateral deflections are produced.

Evaluation Criteria

Two approaches can be used to evaluate the effects of long term loading on capacities. In the first approach, the magnitude of the sustained load under which the wall fails after a specified period of time is determined. In this case, the level of sustained load must be defined and must be greater than the service load to provide a margin of safety against failure. On the other hand, it seem rational that the level of sustained load be less than the factored load because the factored load is not expected to act for the lifetime of the structure.

In the second approach, the residual strength of the wall is determined after a specified period of time under a specified level of sustained load. The sustained load can be taken equal to the service load, similar to the case of defining the serviceability limit. Alternatively, where some loads are unlikely to be sustained (i.e., 100% of live load, snow, or wind), some fraction of the service load could be more appropriate. In this case, the factored load is considered as a short term overloading and because sustained loading is to be expected, the member should be able to carry this factored load and moment after the period of sustained load. Although arguments can be made for walls to withstand some level of sustained overloading, the approach chosen was to study the remaining capacity after some fraction of the service load was sustained for a period of time. It is suggested that this is a more direct approach for defining the long term failure load.

In the Canadian masonry code, CAN3-S304-M84, the effects of the creep on the long term capacities of axially loaded slender members were accounted for in the reduced modulus of rigidity used in the moment magnifier approach. The proposed limit states design code, CSA S304.1-94, uses the reduction factor $(1+\beta_d)$ to reduce the modulus of rigidity where β_d is the ratio of the factored dead load moment to the factored total moment. This ratio was proposed by MacGregor et al. (1970) for reinforced concrete based on the analytical work done by Manuel and MacGregor (1967). The American Concrete Institute adopted this reduction factor in ACI 318-89 and previous editions.

FINITE ELEMENT CREEP SIMULATION

Creep Functions

Test data for 4-block high normal weight masonry prisms (Maksoud 1994) loaded under sustained axial load for almost 400 days were used to develop creep functions. The response which include both the creep in the concrete blocks and the mortar joints is referred to as

global creep whereas the creep of the concrete blocks only is referred to as micro creep. In the finite element model (Maksoud et al., 1992), creep at the integration points which include both block and mortar joints is based on the global creep response whereas the micro-creep is used for integration points which include only blocks.
The following are the creep functions used in the finite element model.
1. Global creep response:

$$\varepsilon_{cr} = F \Lambda_N \left[0.0008\left(\frac{\sigma}{f_c}\right) - 0.000434\left(\frac{\sigma}{f_c}\right)^2\right] \qquad [1]$$

2. Creep in the concrete block (micro creep):

$$\varepsilon_{cr} = F \Lambda_N \left[0.000175\left(\frac{\sigma}{f_c}\right) + 0.000798\left(\frac{\sigma}{f_c}\right)^2\right] \qquad [2]$$

where Λ_N is a modification factor to account for different creep responses for different masonry compressive strengths. In the present study, Λ_N was taken equal to unity because of the close material properties used in the short term analysis and tested prisms. σ is the sustained stress and f_c is the compressive strength of the masonry. F is a logarithmic function expressed as

$$F = 0.64 \log_{10} t + 0.4 \qquad [3]$$

where t is the time in days under sustained load.

Creep Strain Versus Stress Relationship
One way of predicting the creep response under multiaxial states of stress using the creep data from uniaxial test results is to use the principle of effective stress and effective strain along with the strain flow rule in the same manner as in the theory of plasticity. The effective stress is associated with a certain loading or yield function and the effective strain is either defined using the assumption of incompressibility or the equivalent strain energy approach. For simplicity, the creep response is assumed to be pressure independent (Anand et al., 1983 and 1991). Accordingly, Von Mises's yield surface ($F(\sigma_{ij})$) can be used to relate the multiaxial stresses and the creep strains. Based on the definition of the Von Mises yield locus ($F(\sigma_{ij}) = J_2$), the effective stress (σ) can be defined as follows:

$$\sigma = (3 J_2)^{0.5} = \left(\frac{3}{2} S_{ij} S_{ij}\right)^{0.5} \qquad [4]$$

where J_2 is the second deviatoric stress invariant and S_{ij} is the deviatoric stress tensor. Using the incompressibility assumption for the creep strain (Bushnell (1977) , Bathe (1982) and Anand et al. (1983) and (1991)), the effective creep strain can be expressed as:

$$\epsilon = \left(\frac{2}{3}\,\epsilon_{ij}\epsilon_{ij}\right)^{0.5} \qquad [5]$$

where ϵ is the effective creep strain and ϵ_{ij} is the creep strain tensor. Similar to the case of dealing with plastic strain, Eqs. 6.11 and 6.12 along with the associated flow rule result in the creep strain increment (Hill, 1950):

$$\frac{d\epsilon_{creep}}{dt} = \frac{3}{2}\frac{df}{dt}\frac{s_{ij}}{\sigma} \qquad [6]$$

where ϵ_{creep} is the incremental creep strain vector and f is the creep strain-time-stress function (Eqs. 1 to 3). It worth noting that, instead of using real time, the effective time must be used in the creep function by substituting the effective creep strain (Eq. 5) and effective stress (Eq. 4) into the creep function. This is done to relate the elapsed time under the uniaxial stress state, used to develop the creep function, to the elapsed time under the multiaxial state of stress.

Creep Under a General Stress History

Most creep data and mathematical representations were obtained under conditions of constant uniaxial stress over the full test period. Therefore, they usually do not include any provision to rationally account for stress histories. Several methods have been developed to predict creep strain under a general stress history. A comprehensive review of these methods can be found in the book by Neville et al. (1983).

The rate of creep method developed by Glanville in 1930 to rationalize the prediction of the creep under varying stresses (Neville et al., 1983) was used in the present study. This method is based on the assumption of an equal creep rate regardless of the time of application of the load. In other words, for a structure loaded at time t_o, the rate of creep strain due to an additional stress increment at time t depends on the rate of creep at that time which could be very small if the structure was loaded at an old age. Accordingly, under increasing stress, such a method underestimates the creep strain. This technique was initially developed based on a linear stress-creep strain relationship by utilizing the principle of specific creep (creep per unit stress). However, using the equation-of-state approach (MacGregor (1967), Bushnell (1977) and Bathe (1982)) which incorporates comprehensive creep functions, the concept of a constant rate of creep was adopted in the inelastic stages at high stress levels. These functions relate the creep strain with any level of stress in the same way as Eqs. 1 and 2. The simplicity of this technique, as opposed to the difficulties in assigning different parts of the creep response to different creep components in the rate of flow method, and the large memory required to store stress histories for every stress increment at every integration point in the superposition method, is the reason for its use in the present numerical model.

Initial Strain Technique

One of the common approaches to simulate the creep effect, in finite element analyses, is to consider the creep strain as an initial strain in the material which does not produce stress. The

mathematical procedures for the initial strain approach are similar to the experimental procedures which are followed during creep tests. In the initial strain method, the creep strain increment, determined for a specific time increment, produces a stress drop ($d\sigma$) expressed as follows:

$$d\sigma = D\ (\ d\varepsilon_{creep}\ ) \qquad [7]$$

where D is the elasticity matrix, assuming elastic behaviour during the creep unloading. The change in the internal force corresponding to the decrease in stress is

$$dF = \int_v [B]\ d\sigma\ dv \qquad [8]$$

where [B] is the strain-displacement matrix and v is the volume of the specimen. To preserve equilibrium with the external force, a new load increment is applied to compensate for the change in force. This is similar to what happens in a creep test as the load is adjusted back to its original magnitude. The strain and stress due to this load increment have to be added to the values obtained before the current time increment, which is also equivalent to taking the creep strain reading after adjusting the load.

PARAMETRIC STUDY

Parametric studies were conducted on normal weight slender unreinforced walls to determine the residual wall strength after 25 years of sustained loading. This period was chosen because it accounts for most of the creep deformation of masonry materials, similar to concrete (Manuel and MacGregor, 1967). The three major parameters, namely the h/t, e/t and e_1/e_2 ratios, were included in this investigation. The two levels of sustained load chosen were 20% and 40% of the short term capacities (STC) obtained from a previous parametric study (Maksoud et al., 1993).

Loading Sequence

The loading sequence consisted of short term loading which was applied incrementally to the wall until the specified load was reached. As mentioned before, this load was chosen to be 20% and 40% of the short-term capacities (STC). Then the creep analysis was carried out for a period of 25 years, divided into 18 time increments as shown in Table 1. After the period of sustained load, additional short term loading was applied incrementally until failure was identified.

Instead of repeating the numerical procedures, which includes the solution of the equilibrium equation for small time increments, the subincremental technique was used. This allows for determination of the rate of creep depending on the current elapsed time using longer time increments. In the subincremental technique, the specified time increment (7 days for example) is divided equally into subincrements after which the effective time is updated using the current state of stresses and creep strains. Use of 15 subincrements was chosen to be

similar to that used in the plasticity model.

Table 1 Incremental Periods

Number of increments	Period (days)	Total time (days)
7	1	7
3	7	21
3	112	336
5	1752	8760
Total time		9124

Ranges of Parameters and Material Properties

Twenty eight walls were analyzed to investigate practical ranges of the chosen parameters. The two extreme values of e_1/e_2 (1 and -1) were used to represent the cases of symmetric single curvature and anti-symmetric double curvature, respectively. In Table 2, the wall height of 3.6, 4.8, 6.0, 7.2 and 8.4m (11.8, 15.7, 19.7, 23.6 and 27.6 ft) represent slenderness ratios of h/t=18.9, 25.3, 31.6, 37.6, 37.9 and 44.2 for the actual block thickness of 190 mm (7.5 in). For the analyses, the effective mortar bedded area and face shell thickness were based on an average face shell thickness of 34.9 mm (1.55 in). The eccentricity of 20 mm (0.79 in) represents the minimum eccentricity of 0.1 t whereas the 60 mm (2.36 in) value is close to the upper limit of 0.33 t above which flexural tensile strength is a controlling design parameters.

Material properties correspond to masonry assemblage of moderate strength (Guo, 1990) were used. Compressive strengths of 19 MPa (0.13psi), 20 MPa (0.14psi) and 13 MPa (0.09psi) were assigned to masonry prism, standard concrete blocks, and mortar, respectively. These values correspond to compression tests on 4-block high prism, 150 mm high coupon cut from concrete block, and 50 mm high mortar cubes tested using brush end plates. According to the test data (Guo, 1990), the initial moduli of elasticity of the concrete block and mortar joint were taken as 20700 MPa (142.7 psi) and 10000 MPa (68.9 psi), respectively. Poisson ratio of 0.19 was assigned to both blocks and mortar. Also, the corresponding uniaxial stress-plastic strain curves were used in the plasticity model.

Discussion of Results

Figure 1 contains groups of normalized load-deflection curves for 3.6 and 4.8m high walls subject to 60 mm load eccentricity of single curvature. Figures 2 (a) and (b) contain normalized load-deflection curves for 6.0 m high walls under load eccentricity of 60 mm with single and double curvatures. The predicted long term capacities of 28 walls are presented in Table 2. The capacities were normalized by the compressive strength of 4-block high prisms (590 kN (2478 Kips)) predicted by the finite element model and the mid-height deflections

were normalized by the wall thickness (190 mm). The following points provide discussion and interpretation of the above data:

1. For walls deflected in symmetric single curvature (e_1/e_2=1), the reduction in the capacities varied according to the wall heights, (h/t ratios), the load eccentricities (e/t ratios), and the level of sustained loading. In the case of 3.6 m high walls (h/t=18.95), the reductions in the capacities were relatively insignificant ranging from 3% to 7% under different load eccentricities. For the 4.8 m high walls (h/t=24), the reductions in the capacities increased significantly when the level of sustained load increased from 20% to 40% of the short term capacity (STC). In these cases, the reduction in the capacities increased from 6% to 17% in the case of e/t=0.1 and from 10% to 20% in case of e/t=0.3. For the 6.0 m high walls, the reduction was more significant when the level of sustained loading changed from 20 to 40% of the short term capacity (STC). These reductions changed from 2% to 9% and from 10% to 30% for e/t ratios of 0.1 and 0.3, respectively. As can be noted, the wall heights had significant roles in intensifying the effect of the creep strains. This can be seen in Figs. 1 to Fig. 3 where the creep deflections under sustained load of 40% of the short term capacities and e/t=0.3 were almost two, three, and four times the creep deflections under sustained load of 20% of the short term capacities for 3.6m, 4.8m, and 6.0m high walls, respectively. These ratios decreased slightly for e/t =0.1.

Table 2 Normalized† Long-Term Capacities of 190 mm Hollow Block Walls

e_1/e_2 ratio	Wall height (m)	Capacity for Sustained Loads Expressed as Ratio of the Short Term Capacity					
		Eccentricity=20 mm			Eccentricity=60 mm		
		0.00	0.20	0.40	0.00	0.20	0.40
1	3.6	0.70	0.68	0.64	0.50	0.48	0.47
	4.8	0.63	0.59	0.52	0.43	0.39	0.34
	6.0	0.53	0.52	0.48	0.34	0.31	0.24
-1	4.8	0.81	0.79	0.79	0.63	0.60	0.57
	6.0	0.69	0.66	0.69	0.60	0.57	0.57
	7.2	0.63	0.63	0.63	0.55	0.52	0.52
	8.4	0.56	0.56	0.53	0.51	0.51	0.49

† Normalization by dividing by $f'_m A_n$ where f'_m=19 MPa (2775 psi)
Conversion 1 in=25.4 mm, 1 ft=0.305 m

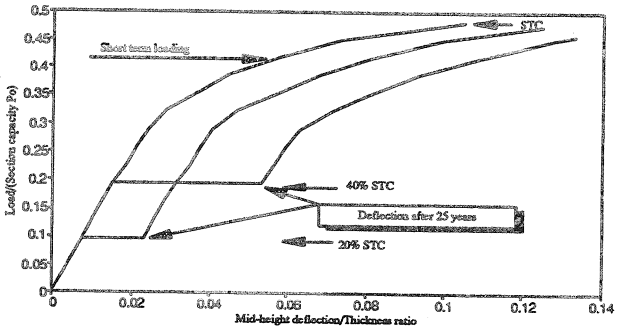

(a) 3.6 m High Walls

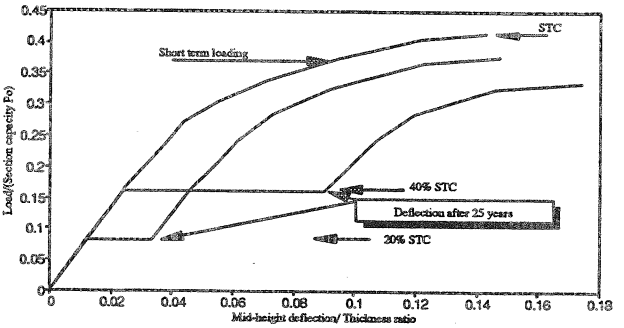

(b) 4.8 m High Walls

Fig. 1 Short and Long Term Behaviour of 190 mm Hollow Block Walls Under Symmetric Single Curvature and e=60 mm.

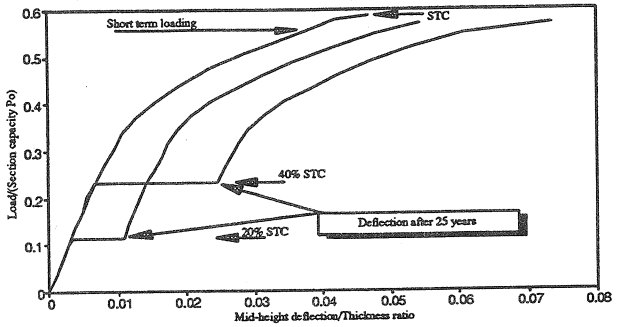

(a) Symmetric Single Curvature (e_1/e_2=1)

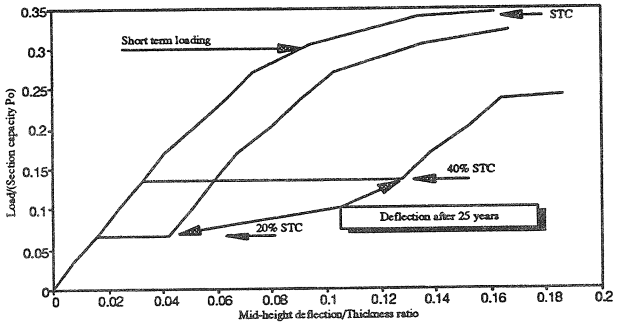

(b) Anti-Symmetric Double Curvature (e_1/e_2=-1)

Fig. 2 Short and Long Term Behaviour of 6.0 m High and 190 mm Hollow Block Walls with Eccentricity of 60 mm

2. It is quite clear from Table 2 that changing the deflection mode from symmetric single

curvature (e_1/e_2=1) to double curvature (e_1/e_2=-1) had a remarkable effect on reducing the creep effect in most situations. The average reduction in the capacities dropped to 3 and 5% for e/t equal to 0.1 and 0.3, respectively under sustained loading of 40% of the short term capacity. Therefore, it can be concluded that under the whole ranges of slenderness and eccentricities/thickness ratios, the long term capacities are nearly the same as the short term capacities for walls under e_1/e_2=-1. The minor effect of creep for the case of e_1/e_2=-1 can be explained using Fig. 4 where it can be seen that the added creep deflections, even under e/t =0.3, are only a few millimetres which did not produce significant secondary moments. The same response was reported by MacGregor et al. (1970) regarding reinforced concrete columns bent in double curvature.

3. Although the creep strains produced additional lateral deflections, some walls subjected to double curvature had long-term capacities as high as the short term capacities. In the case of the small eccentricity ratio (e/t=0.1), this response can be attributed to the additional deflection due to the creep which enhanced the second buckling mode. This may delay the transfer from the double curvature mode to the single curvature mode, resulting in higher capacities. For the higher eccentricity ratio (e/t=0.3), the comparable capacities can be attributed to the fact that critical sections are close to the wall ends near the locations of the maximum primary moment where the P-δ is not significant. The same response in the case of double curvature situations was reported by Manuel and MacGregor (1967) regarding reinforced concrete columns.

PROPOSED EI REDUCTION FACTOR

Moment magnifier approach has been successfully used to account for secondary moments in reinforced concrete as well as masonry members subject to axial loads and out-of-plane bending. To account for inelastic material response, cracking, and creep effects, effective modulus of rigidity EI_{eff} has to be developed to empirically fit the behaviour of the walls. The finite element results for the long term loading were used for this purpose. According to the moment magnification factor formula, the reduction factor R for the elastic uncracked modulus of rigidity ($EI_{elastic\ uncracked}$) can be expressed as

$$R = \frac{EI_{eff}}{EI_{elastic\ uncracked}} = \left(\frac{h}{\pi}\right)^2 \frac{G}{G-1} \frac{\beta}{EI_{elastic\ uncracked}} \qquad [9]$$

where h is the wall height, G is the moment magnification factor, and β is the normalized wall capacity (Table 2). Using the moment-thrust interaction diagram of a short wall, the moment magnification factor G can be determined by dividing the moment capacity of the short wall at peak load by the primary moment capacity. Using the long term wall capacities corresponding to sustained loads of 40% of the short term capacities and neglecting the creep effect in the case of antisymmetric curvature, a formula for the reduction factor R was developed using stepwise regression and was expressed as

$$R = 0.2438 + 0.00472 \frac{e}{r} \frac{h}{r} \qquad [10]$$

with R-SQ equal to 87%, where R-SQ is equal to the sum of the squares of R values due to regression divided by the sum of squares of R values predicted using finite element results (Eq. 9). r is the radius of gyration of the cross section. As can be noted from Eq. 10, the EI reduction factor R increases as e/r and h/r increase. Similar to the reduction factors developed from short term loading (Maksoud et al., 1993), this response can be attributed to the inelastic material responses associated with walls of low e/r and h/r ratios, where more reduction in the elastic uncracked modulus of rigidity is needed for shorter walls with low h/r ratios.

REFERENCES

ACI 530/ASCE 5/TMS 402, (1992) "Masonry Standard Joint Committee" Building Code Requirements for Masonry Structures, American Concrete Institute, Detroit, American Society of Civil Engineering, New York, The Masonry Society, Boulder.

Anand, S.C. and Gandhi, A. , (1983), "A Finite Element Model to Compute Stresses in Composite Masonry Walls due to Temperature, Moisture and Creep" Proc., Third Canadian Symposium.University of Alberta, Edmonton, Alberta, Canada, pp.34-1.

Bathe, K.J., (1982)," Finite Element Procedures in Engineering Analysis" Prentice-Hall, Inc., Englewood Cliffs, New Jersy.

Ben-Omran, H. and J.J. Glanville (1989) " Strength of Reinforced Masonry Columns Under Sustained Load" 5th Canadian Masonry Symposium, University of British Columbia, Vancouver, B.C, Canada.

Bushnel, D. (1977), " A Strategy For The Solution of Problems Involving Large Deflection, Plasticity, And Creep" International Journal for Numerical Method in Engineering Vol. 11, pp. 683-768 .

Maksoud, A. and Drysdale, R.G. (1992)," Numerical Modelling of Masonry Wall" The 6th Canadian Masonry Symposium, Saskatoon, Saskatchewan, June 15-17, pp. 801-811.

Maksoud, A. and Drysdale, R.G., (1993), " Rational Moment Magnification Factor for Slender Unreinforced Masonry Walls" The 6th North American Masonry Conference Philadelphia, Pennsylvania, The Masonry Society, June 6-9, pp.443-454.

Maksoud, A. (1994), "Short and Long Term Capacities of Slender Concrete Block Walls" Ph.D. thesis, McMaster University, Hamilton, Ontario.

Manuel, R.F. and MacGregor, J.G. (1967), " Analysis of Reinforced Concrete Column Under Sustained Load", ACI Journal, January, pp. 12-23.

Neville, A.M, Dilger, W.H., and Brooks, J.J., (1983), " Creep of Plain and Structural Concrete" Construction Press, London and New York .